A PULSAR EMISSION MECHANISM

by

F. C. Michel and W. H. Tucker

Department of Space Science
Rice University
Houston, Texas 77001

DEPARTMENT OF

SPACE SCIENCE

RICE UNIVERSITY

HOUSTON, TEXAS

A PULSAR EMISSION MECHANISM

by

F. C. Michel and W. H. Tucker

Department of Space Science
Rice University
Houston, Texas 77001

February 1969

A PULSAR EMISSION MECHANISM

F. C. Michel and W. H. Tucker
Department of Space Science
Rice University
Houston, Texas 77001

We point out that the interaction between two basic types of plasma discontinuities in relative motion, namely the tangential and shock discontinuities, should result in pulsed emission of electromagnetic radiation. These discontinuities are both observed in the interplanetary plasma flow. Currents must flow on these discontinuities, and the radiation is generated by the acceleration of these currents at the intersection points of the shock and tangential discontinuities. Under conditions thought applicable to pulsars, NP 0532 (the pulsar associated with the Crab Nebula) would radiate about 4×10^{30} erg/sec of radio energy below about 10^{3} MHz. The efficiency of this mechanism is quite low ($\sim 10^{-8}$ for NP 0532) for the assumed conditions, and direct extention to the much slower pulsars would require that they have moments of inertia much larger than attributable to neutron stars.

The basic purpose of this letter is to propose a mechanism for pulsar radiation. We also offer a relationship, based on this mechanism, that appears to be satisfied by the pulsar associated with the Crab Nebula. It is necessary in any very specific discussion to adopt some basic model for the pulsar. We have argued (Tucker and Michel 1968) that (1) the pulse repetition represents rotation of (2) a very condensed object (e.g., neutron star), with (3) the radiation being associated with neutral surfaces in the pulsar magnetosphere. Gold (1968) has independently forwarded the first two suggestions (c.f. Maran and Cameron 1968) and we wish to discuss a possible mechanism (point 3) and its consequences in more detail here.

The pulsar associated with the Crab Nebula (NP 0532) is observed to be slowing down with an e-folding period of about 2×10^3 years (Craft et al. 1968), and, even for a neutron star, the resultant rotational energy loss rate must be comparable to the luminosity of the entire nebula (Finzi and Wolf 1968). The observed slowing down implies a large torque, and a well-known mechanism for such a torque is mass loss in the presence of a strong magnetic field. In the case of the sun, the outward flow of plasma carries out solar magnetic field lines (hence the plasma flows faster than the local Alfvén velocity) to form a predominantly radial magnetic field structure. Rotation of the sun causes the field lines to take the form of Achimedian spirals (c.f. Parker 1963). The radial extension of the solar magnetic field transfers angular momentum to the outflowing plasma and thereby results in a significant angular momentum loss by the sun (Dicke 1963; Modisette 1967; Weber and Davis 1967). The angular momentum loss is a factor of 10^3 greater than that expected if the effects of the magnetic field were neglected.

We have enough information at hand to estimate the field and plasma flow for NP 0532 on the basis of the above model. Corotation can take place out to a radial distance of at most

$$R_o = c/\omega_o, \tag{1}$$

which for NP 0532 is about 1.5×10^8 cm ($\omega_o = 2 \times 10^2$ radians/sec). The torque is of the order of

$$\text{Torque} = \frac{dM}{dt} R_o^2 \omega_o \tag{2}$$

giving, for either the energy loss rate estimated by Finzi and Wolf (1969) or the observed luminosity of the Crab of $\approx 10^{38}$ erg/sec (Haymes <u>et al.</u> 1968),

$$\frac{dM}{dt} \approx 10^{17} \text{ g/sec}, \tag{3}$$

which for near-relativistic flow velocities corresponds to a density near the corotation limit of

$$\rho \approx 10^{-11} \text{ g/cm}^3. \tag{4}$$

For corotation to actually be effective out to R_o, the azimuthal component of the Alfvén velocity must be comparable there to the velocity required for rigid corotation (Modisette 1967), or

$$B_o \ (\mu_o \rho)^{-\frac{1}{2}} \approx c. \qquad (5)$$

Thus,

$$B_o \approx 3 \times 10^5 \text{ gauss}, \qquad (6)$$

which corresponds to a trapped flux inside a pulsar object 10 km in radius of 2×10^{22} gauss-cm^2 essentially equal to that for the sun. The magnetic field is radial ($B \propto 1/r^2$) for $r \ll R_o$ and becomes azimuthal ($B \propto 1/r$) for $r \gg R_o$ as shown in Figure 1, whereas the flow is very nearly radial at large distances ($\rho \propto 1/r^2$). Since the net magnetic flux out of any closed surface must be zero, regions of both outward and inward radial flux must be present, which therefore are separated by surfaces of zero radial flux (neutral surfaces, or tangential discontinuities in general). These discontinuities are observed in the interplanetary medium (c.f. Siscoe et al. 1968) and the minimum thickness of these sheets is of the order of the ion cyclotron diameter. The proton energies will be on the order of 10^9eV for the above magnetic field strength (stronger fields would result in more energetic particles and require, for a given torque, a proportionately smaller particle loss rate) and therefore the cyclotron radius for either protons or electrons of that energy is

$$a_c \sim 10 \text{ cm}. \tag{7}$$

We now show that, given this model, a certain part of the energy loss will be in the form of pulsed, linearly polarized, low frequency ($\lesssim 10^9$ Hz) electromagnetic radiation. Most of the energy loss is initially in the form of outflowing magnetized plasma; however, we note that (1) the tangential discontinuities delineate rapid changes in field direction and (2) the magnetic field drops off as 1/r. In other words, we already have very nearly a pulsed radiation field. A shock transition must exist at some large radial distance to slow the flow to submagnetoacoustic velocities in response to the surrounding medium. The intersection of each neutral sheet with the shock transition causes the surface currents flowing on these two discontinuities to undergo rapid changes in velocity and magnitude. The shock-neutral sheet interaction should therefore be a source of electromagnetic radiation. This mechanism will be examined in detail elsewhere (Michel and Wolf 1969). Figure 2 shows the geometrical relationships among the various discontinuities and the radiation pulse that emanates from their interaction. It is straightforward to estimate the radiated intensity and spectral distribution since the pulse amplitudes will be comparable to the ambient field amplitudes but, for a fixed observer, will be of duration $\Delta t \sim 2\, a_c/c$. The radiated energy is therefore essentially the fraction of the energy flux within neutral sheets, or

$$L_{radio}/L_{rotation} \sim 2\ a_c/\pi R_o = 2\ \omega_o/\omega_{max}. \qquad (9)$$

For $a_c = 10$ cm, $R_o = 1.5 \times 10^8$ cm, and $L_{rotation} = 10^{38}$ erg/sec, we obtain

$$L_{radio} \sim 4 \times 10^{30} \text{ erg/sec}, \qquad (10)$$

in accord with the observed luminosity for NP 0532 (our value for a_c is only an order-of-magnitude estimate). We have shown elsewhere (Michel 1969) that the quantity a_c/R (the neutral sheet thickness divided by the spacing between neutral sheets) remains constant despite expansion and energy loss from the plasma. The resultant constancy of the pulse width together with $B \sim 1/r$ means that the pulsed radiation output is insensitive to the location of the shock; we would expect such a shock to be many A.U. from the pulsar object. The frequency spectrum will simply be the Fourier transform of a pulse of duration Δt, which for a smooth (e.g. gaussian) shape is constant at very low frequencies and drops off sharply at higher frequencies (around 10^9 Hz), as seems to be observed for the pulsars.

We are only radiating rotational energy in the above model, thus we can regard the moment of inertia as the only unknown and solve for it, using equation (9), in terms of observable quantities. Thus,

$$I = I_o F_\nu (\int n_e d\ell)^2 \nu_c^2 P^3 T / \langle n_e \rangle^2 \qquad (11)$$

where I_o is a proportionality factor, F_ν the flux density at low frequency, $\int n_e d\ell$ the dispersion measure, ν_c the cutoff frequency (adopted to be frequency at which flux density drops to 1/e), P the pulse period, T the effective lifetime $(P/\dot{P})$, and $\langle n_e \rangle$ is the average electron concentration in the direction of observation. Table 1 shows the assumed values and resultant moments for those pulsar with measured values of T. The agreement among the first three is certainly adequate, especially since CP 1919 is close to the galactic plane (4°) and is perhaps relatively closer. The usual views regarding compact stars argue that electron-degenerate stars should have moments of inertia exceeding about 10^4 I_o while nucleon-degenerate stars should have moments less than or about I_o ($I_o \approx 1.2 \times 10^{45}$ g cm^2 in equation (11) for the units indicated in Table 1). Thus, while the first three pulsars could be regarded as electron-degenerate stars, CP 0950 would either have to be 10 times closer than the rest (to be a neutron star of conventional design) or have a mass-radius relationship not thought to be stable. Possibly rotational effects play a major role in the stability of these objects. Any rotational model must face up to substantially the same difficulty: if all pulsars are substantially the same and the slowing down is proportional to the radio luminosity, then the Crab pulsar is anomalously dim. Furthermore if they are all neutron stars, the conversion efficiency into radio pulses must be near 100% (except again for NP 0532).

In the spirit of such short communications, we defer the discussion of many important questions, such as the morphology of the pulse features and the relevance of NP 0532 to the Crab Nebula as a whole, although it has already suggested that neutral sheet structures within the volume of the Nebula are essential to the observed synchrotron radiation (Michel 1968, 1969). The observed pulse width can be understood in terms of perturbations to the shock position and shape, and so on; the only basic difficulty encountered has been the moment of inertia question outlined above.

We wish to acknowledge the interest and encouragement by A. J. Dessler, and the many valuable comments by R. A. Wolf. This work was supported in part by NASA under Grant No. NGR-44-006-033.

TABLE 1

Moment of Inertia determined from equation (11). The units are 10^{-26} J/m^2 Hz (at 81.5 MHz), electrons-parsec/cm^3, 100 MHz, seconds, and 10^7 years respectively. The quantity I_o is then 1.2×10^{45} g cm^2, and we assume an average electron concentration of 0.1 electron/cm^3. Data is from Ekers and Moffett (1968); Staelin and Reifenstein (1968); Rickett and Lyne (1968); Maran and Cameron (1968).

Pulsar	$F_{81.5}P$	$\int n_e d\ell$	ν_c	P	T	I/I_o
CP 1919	0.55	12.5	5	1.337	4.2	16×10^3
CP 0834	0.4	12.8	3	1.274	0.7	7×10^3
CP 1133	0.4	4.9	7	1.188	1.0	7×10^3
CP 0950	0.2	3.0	6	0.253	3.0	124
NP 0532	0.3*	56.0	10**	0.033	0.00024	0.3

* Only individual pulses brighter than about 10 in these units are visible above the Crab background. These pulses are quite infrequent, and therefore the average flux should be considerably less as indicated by this rough estimate from very limited data.

** Assumed -- actual measurements either unknown or unavailable.

CAPTIONS

Figure 1. Spiral magnetic field structure in the plasma flow away from the proposed pulsar model as seen in the equatorial (rotation) plane. The plasma flow is essentially radial everywhere. The shock transition is shown much too close on the scale of this figure, and a neutron star would be smaller than the central dot. The shaded area is illustrated in Figure 2, except that here the inward pulse has been omitted in an attempt to simplify this figure.

Figure 2. Passage of a neutral sheet through a shock transition, illustrated for a compression factor of 3 and an incident flow velocity of 0.9 c. Sheet currents flow to maintain the change in sign of $\underline{B}$ across the neutral sheet and the change in magnitude of B across the shock. The acceleration of these currents generates the radiation pulse. This pulse is polarized parallel to the surface current direction ($\underline{E}$-vector perpendicular to the plane of the figure) and is analogous to Čerenkov radiation in that the phase velocity of the intersection between the neutral sheet and the shock moves

very much faster than c, giving a shock-wave like form to the radiation pulse. Equivalently, it could be regarded as coherent bremsstrahlung generated by the change in direction of the current carriers (the current flowing on the shock surface changes sign), which allows the polarization sense to be more readily appreciated.

REFERENCES

Craft, H. D., Jr., Lovelace, R. V. E., Richards, D. W., and Sutton, J. E. 1968, to be published.

Dicke, R. H. 1964, Nature, 202, 432.

Ekers, R. D. and Moffett, A. T. 1968, Nature, 220, 756.

Gold, T. 1968, Nature, 218, 731.

Haymes, R. C., Ellis, D. V., Fishman, G. J., Kurfess, J. D., and Tucker, W. H. 1968, Ap. J. (Letters), 151, L9.

Maran, S. P. and Cameron, A.G.W. August 1968, Physics Today, 21, 8, 41.

Michel, F. C. 1968, J. Geophys. Res., 73, 4135.

Michel, F. C. 1969, Ap. J., to be published.

Michel, F. C. and Wolf, R. A. 1969, in preparation.

Modisette, J. L. 1967, J. Geophys. Res., 72, 1521.

Parker, E. N. 1963, Interplanetary Dynamical Processes (New York: Interscience Publishers), Ch. 10.

Rickett, B. J. and Lyne, A. G. 1968, Report presented at the Fourth Texas Symposium on Relativistic Astrophysics, Dallas, Texas, 16-20 December.

Siscoe, G. L., Davis, L., Jr., Coleman, P. J., Jr., Smith, E. J., and Jones, D. E. 1968, J. Geophys. Res., 73, 61.

Staelin, D. H. and Reifenstein, E. C., III 1968, Science, 162, 1481.

Tucker, W. H. and Michel, F. C. 1968, Report presented at Conference on Pulsars, New York, N. Y., 20-21 May 1968. See Maran, S. P. and Cameron, A.G.W. loc. cit.

Weber, E. J. and Davis, L., Jr. 1967, Ap. J., 148, 217.

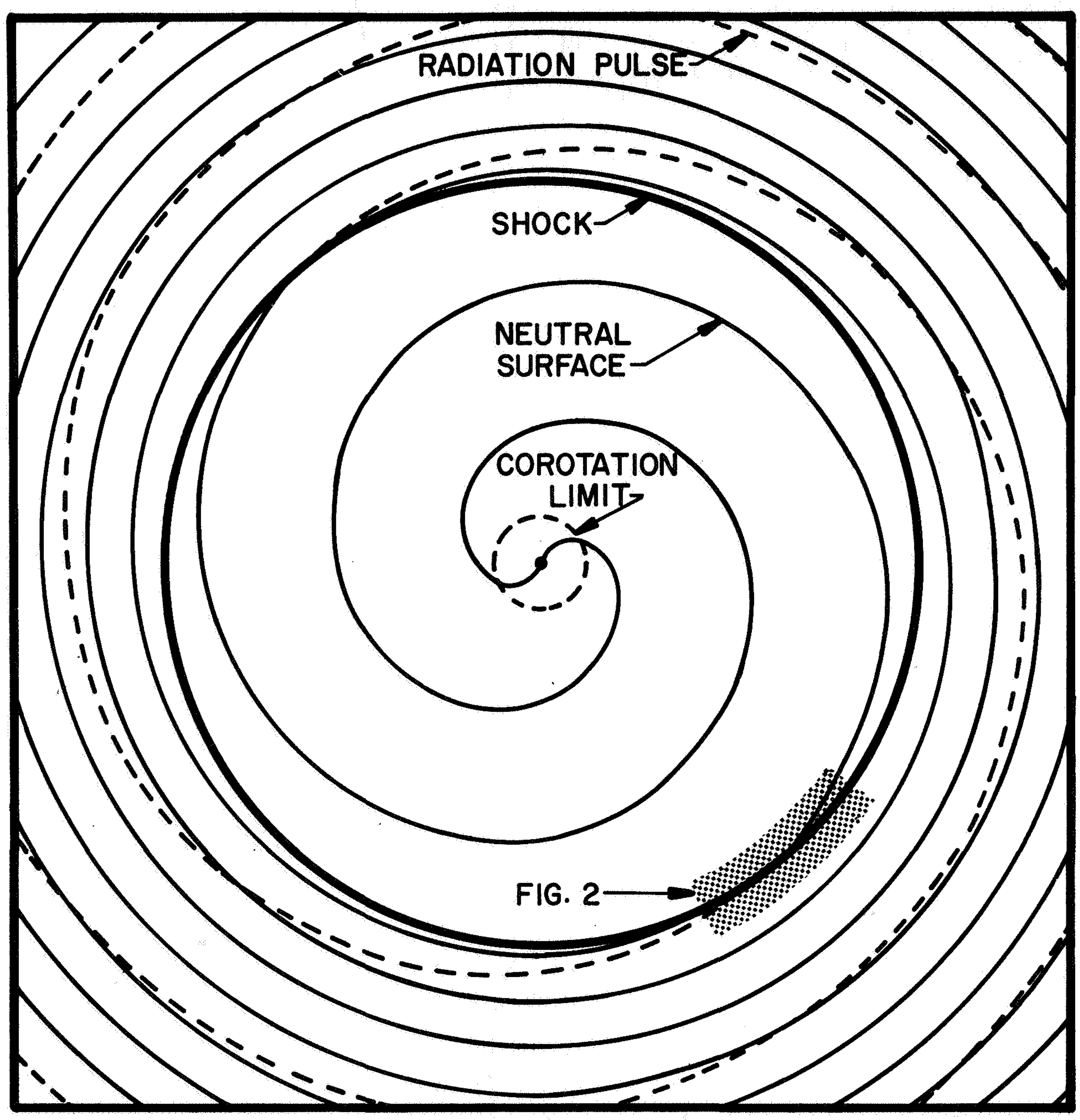
RADIATION PULSE
SHOCK
NEUTRAL
SURFACE
COROTATION
LIMIT
FIG. 2

FIGURE I

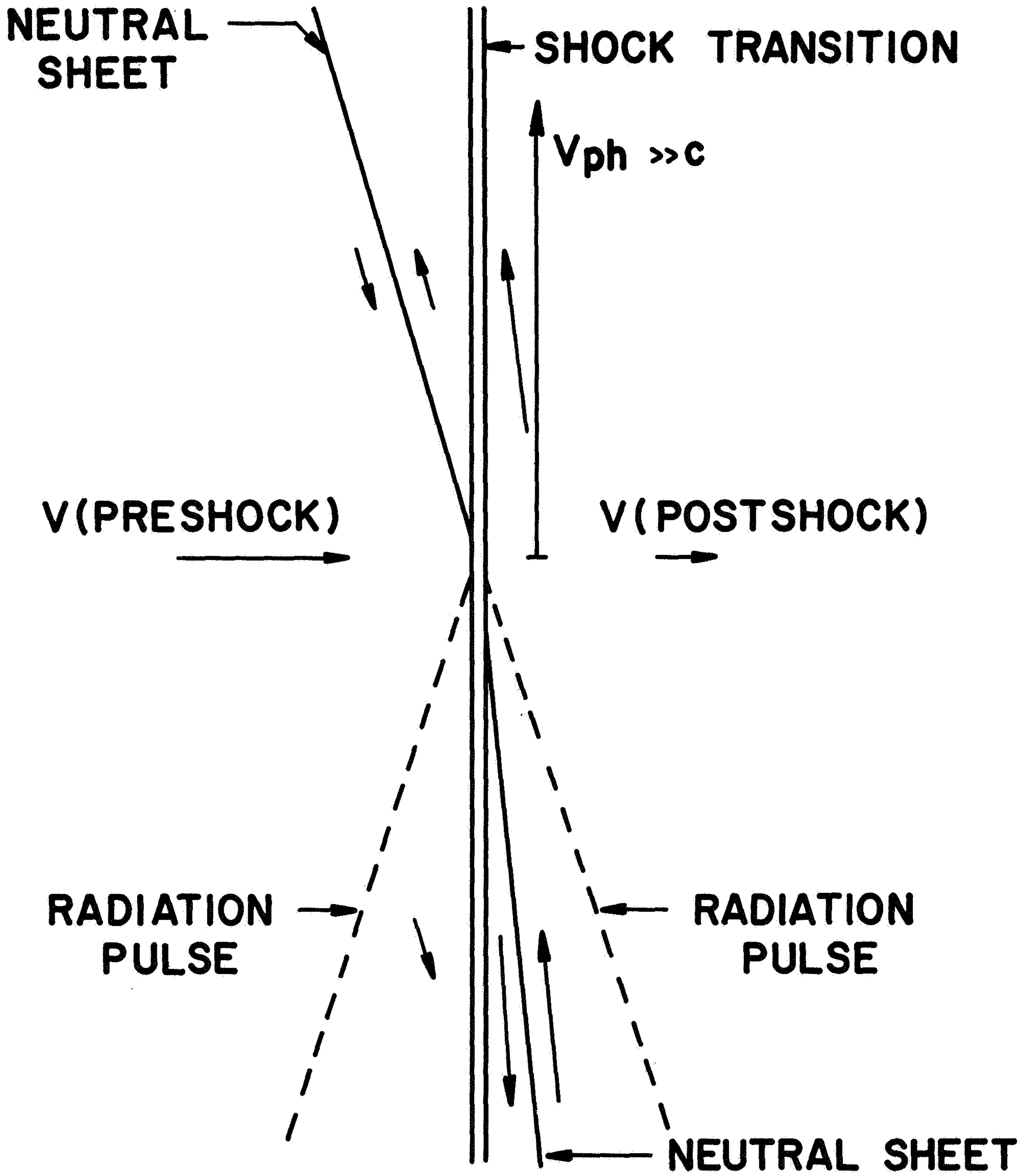
NEUTRAL SHEET
SHOCK TRANSITION
$V_{ph} \gg c$
V(PRESHOCK)
V(POSTSHOCK)
RADIATION PULSE
RADIATION PULSE
NEUTRAL SHEET

FIGURE 2